American Journal of Engineering Research (AJER) 2023
American Journal of Engineering Research (AJER)
e-ISSN: 2320-0847 p-ISSN : 2320-0936
Volume-12, Issue-11, pp: 61-74
www.ajer.org
Research Paper Open Access

Energy analysis of the heat pump operating with supercritical CO_2 driven by thermal compression.

Hossein FALLAHSOHI [a,*]
[a] BOOSTHEAT, 41-47 Boulevard Marcel Sembat, Vénissieux, F-69200, France

Abstract: *One way for reducing energy consumption is to recover energy from the environment using a heat pump. However, the energy for the compressor of electric heat pumps is mainly provided by electricity, which has associated energy losses during its production, transmission, and distribution. This present study considers an alternative approach where the compression is carried out by thermal energy generated through the combustion of a gaseous fuel. Improving the performance of this compressor depends on its design and the efficiency of heat exchange between CO_2 and the heat source. This case study utilizes experimental analysis and modeling to explain and characterize the functioning of a thermal compressor in a heat pump system.*
Keywords: *heat pump, heat source energy, natural gas, supercritical CO_2, energy analysis*

Date of Submission: 12-11-2023 Date of acceptance: 28-11-2023

Nomenclature

COP	Heat pump Coefficient of Performance	η_{mec}	Mechanical efficiency
EHP	Electric Heat Pump	η_{tot}	Total energy efficiency
G_{HP}	Primary energy gain factor	η_{wh}	Efficiency to recover the waste heat
GEHP	Gas driven Engine Heat Pump	ε	Heat exchanger efficiency
GEU	Gas Utilization Efficiency	τ	Pressure ratio
GSHP	Gas Sorption Heat Pump	*Subscripts*	
GTHP	Gas driven Thermal compression Heat Pump	*asp*	aspiration
GWP	Global Warming Potential	*B*	Buffer
HP	High Pressure (bar)	*dis*	discharge
LP	Low Pressure (bar)	*evap*	Evaporator
m	Mass (kg)	*ext*	Exterior
n	Total Number of Stages	*gc*	Gas cooler
P	Pressure (bar)	*HP*	Heat pump
PER	Primary Energy Ration	*HS*	Heat Supplied
PLR	Partial Load Ratio	*in*	inlet
$\dot{\boldsymbol{Q}}$	Heat flow (kW)	*opt*	*optimum*
Q_C	Heat recovered from the environment (kWh)	*out*	Outlet
Q_P	Primary energy (kWh)	*sat*	saturation
Q_{HP}	Thermal energy produced by HP (kWh)	*W*	Water
SPF	Seasonal Performance Factor	*WB*	Water box
$\dot{W}_{elec}$	Electrical power (kW)	*EV*	Exhaust valve
W_{HP}	Electrical energy (kWh)	*IV*	Inlet valve
η_c	Conventional heating system efficiency		

* Corresponding author.
E-mail address: hossein.fallahsohi.ext@boostheat.com

I. Introduction

In recent years, researchers have been working on solutions to reduce the environmental impact of energy systems. One of the solutions that can be used to reduce greenhouse gas emissions is to increase the efficiency of energy systems, particularly in the HVAC sector. A heat pump allows heat to be extracted from a cold source and transferred to a hot source via a compressor that circulates refrigerant between the two sources. On the one hand, this compressor is driven by an energy vector, which is mainly electricity. However, the production of electricity consumes primary energy, which must be considered for energy, exergy, economic and environmental analysis. On the other hand, the conventional refrigerants used in HVAC systems have a high global warming potential (GWP). Due to restrictions imposed by international climate change conferences, there are limitations on the use of high GWP refrigerants [1]. Due to the expected limitations, it is recommended to use low-GWP refrigerants. There are studies on the properties of both natural and synthetic refrigerants that allow the replacement of low-GWP refrigerants with higher-GWP refrigerants. [2]– [5]. By changing refrigerant, obviously due to that the energy efficiency of heat pumps as a refrigeration system changes. Consequently, the replacement of a refrigerant by another can only be relevant if the latter offers better energy consumption or is comparable to the existing one. Therefore, the first step can be to choose a refrigerant. CO_2 can be chosen as a natural refrigerant thanks to its attractive properties [6] : it is close to a perfect gas, environmentally friendly, safe, cheap, and more compact in terms of component and pipe dimensions [7]. In addition, CO_2 is non-toxic, non-flammable, compatible with materials and various oils used in the refrigeration industry. The critical temperature of CO_2 is low (30.98°C) [8] . The thermodynamic cycle by circulating CO_2 as the primary fluid is often transcritical because of its low critical temperature. The properties of supercritical fluids are different from those of a gas or a liquid but are included between them (Table 1). Their viscosity is close to that of a gas, their density is close to that of a liquid, and their diffusivity is very high compared to that of a liquid, which facilitates their penetration into porous media.

Fluid stat	Density [kg/m^3]	Viscosity [μ Pa. s]	Diffusivity [cm^2.s^{-1}]
Gas	0.6 to 2	10 to 30	0.1 to 0.4
Supercritical	200 to 500	10 to 30	0.5×10^{-3} to 4×10^{-3}
Liquide	600 to 1600	200 to 3000	0.2×10^{-5} to 2×10^{-5}

Table 1.Comparison of the orders of magnitude of the properties of a fluid in gaseous, supercritical, and liquid states ([9], [10]*).*

The CO_2 transcritical cycle operates at high pressures, while its compression ratio is lower than a subcritical cycle with other refrigerants at equivalent working conditions [11]. High working pressure, which leads to an increase in compressor performance due to lower compression ratio, as well as it allows to reduce the size of the system. In fact, two factors reduce the size of the system, one is the high working pressure and the other is the low molar mass of CO_2. The high pressures result in high latent heat of vaporization and volumetric heat transfer, and the low liquid to vapor density ratio results in high heat transfer rate [12]. In this state, the viscosity is low, so the pressure drop during heat transfer can be ignored. Despite these advantages of the transcritical cycle, working at high pressures can also lead to disadvantages as the irreversibility loss in expansion processes increases. Thus, in a basic cycle, the loss of exergy in the throttle valve of a transcritical cycle of CO_2 is higher than that of other refrigerants [13]. To improve the performance of the transcritical cycle of CO_2, i.e., to reduce the exergy loss, various modifications of the basic cycle are possible: internal heat exchangers (IHX), ejectors, expanders, subcooling, flash gas bypass, parallel compression, two-stage compression, evaporative cooling, and CO_2-based mixtures. [14]. Therefore, the modified configuration of a heat pump operating with the transcritical CO_2 cycle can be improved and thus compete with those operating with conventional refrigerants.

The non-flammability of CO_2 as a refrigerant makes it possible to use primary energy such as natural gas or waste heat in a heat pump whose compressor operates on thermal energy. This article presents the application of thermal compression in a heat pump. Through modeling and experimentation, the behavior of the system, including the thermal compressor, is analyzed, and explained to enhance its operation.

II. Energy chain of TDHP

A heat pump is a system that extracts heat from the surrounding environment and transfers it to the desired location via a compressor. This method is more efficient than systems that generate heat through fuel combustion or the Joule effect. However, the compressor in a heat pump requires energy and is usually powered by electricity. Therefore, when evaluating a heat pump, it is important to consider both its heating efficiency and energy consumption. The first aspect of concern pertains to the environmental impact arising from the consumption of primary energy, its transmission and distribution, and its conversion for operating a heat pump,

as well as the usage of the refrigerant. The second aspect deals with the energy efficiency of a heat pump. Analyzing an energy chain precisely assesses the two aspects mentioned above.

The energy chain refers to the flow of energy from primary sources to useful energy. Undoubtedly, in this process, there will be losses associated with the conversion, transmission, and distribution of energy. Traditional power plants typically convert only about 30% of the available energy from a fuel into electrical power. Highly efficient combined-cycle power plants convert approximately 50% of the available energy into electrical power[15] . The chemical energy used in the power plant is the primary energy source for the electric heat pump. The lower heat value (LHV) of fuels like natural gas can be used to estimate this energy. Figure 1 displays the energy system's chain.

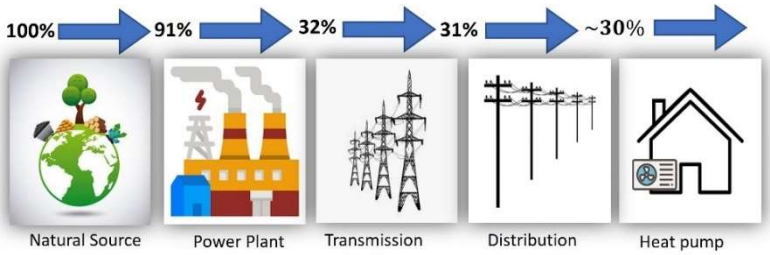

Figure 1. Chain of energy for electric heat pump

The primary energy Q_P that is used to convert to the electricity W_{HP} required to operate the electric heat pump is defined as in Eqs. 1:

$$Q_P\,[kWh] = \frac{W_{HP[kWh]}}{\eta_{tot}} \tag{1}$$

Where η_{tot} is total energy efficiency of the energy chain, including power plant losses and transmission and distribution losses within the network.

Emphasizing that an electric heat pump is a system that converts electricity to heat Q_{HP}, the coefficient of performance is defined as Eqs. 2:

$$COP_{HP} = \frac{Q_{HP[kWh]}}{W_{HP[kWh]}} \tag{2}$$

Q_P the primary energy consumed by an electric heat pump is obtained from Eqs.1 and 2:

$$Q_P\,[kWh] = \frac{Q_{HP[kWh]}}{\eta_{tot}\,.\,COP_{HP}} \tag{3}$$

As stated in Eq.4, The product $\eta_{tot}\,.\,COP$ represent the primary energy ratio (PER), which is the ratio of useful energy output to total energy input:

$$PER_{EHP} = \eta_{tot}\,.\,COP \tag{4}$$

Consequently, it is possible to estimate the primary energy gain factor of a heat pump G_{HP} , by comparing it with a conventional heating system like electric heating or fuel boilers:

$$G_{HP} = \frac{PER}{\eta_c.\eta_p} - 1 \tag{5}$$

Where η_c represents the energy efficiency of a conventional heating system. An electric heater is considered to have a η_c value of 1, while a fuel boiler ranges between 0.5 to 0.95 depending on the fuel boiler [16]. Also, η_p represents the efficiency of the system that converts the primary energy into the input energy vector for the conventional system. For example, for an electric heater $\eta_p = \eta_{tot}$, while for a fuel boiler that directly consumes primary energy, $\eta_p = 1$.

Now the thermal driven heat pump (TDHP) can be compared to the electrically driven heat pump. According to the energy chain illustrated in Figure 2, primary energy can be utilized directly in the TDHP.

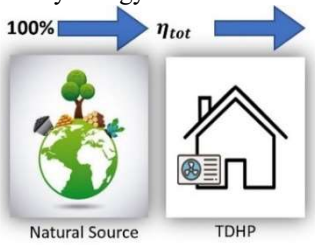

Figure 2. Chain of energy for TDHP

Natural gas is presently the main source of energy used in thermal-driven heat pump systems.
The gas driven heat pump systems can be categorized into three main types: gas-driven sorption heat pumps (GSHPs), gas-driven engine heat pumps (GEHPs) and gas-driven thermal compression heat pumps (GTHPs).
GSHP: The PER of a sorption heat pump can be as high as 1.4, depending on the technology [17]. The COP is measured under nominal conditions during laboratory tests. The heat pump's performance is heavily influenced by the source's characteristics and thermal load [18]. So, for a more objective evaluation, it is necessary to use the Seasonal Performance Factor (SPF), which is the ratio of delivered useful energy to consumed driving energy for the heat pump. A quantitative comparison elucidates the benefit of a sorption heat pump. It is assumed that the thermal machines operate between two identical sources Figure 3.

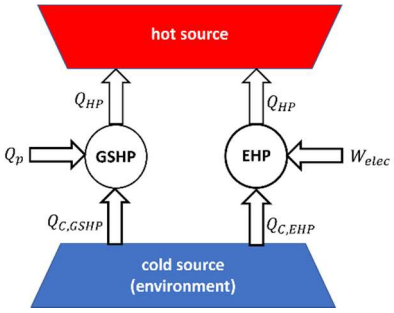

Figure 3. Schematic representation of GSHP and EHP.

Considering that the plant supplies electricity to electric heat pump (EHP) at the end of the energy chain with a total efficiency of 40% and SPF of this heat pump is 3.5, it can be concluded that the SPER will be:

$$SPER_{EHP} = \eta_{tot} \,.\, SPF_{EHP} = 0.4 \times 3.5 = 1.4 \quad (6)$$

SPF_{EHP}	3.5
$W_{elec}\,[kWh]$	3.43
$Q_{HP}\,[kWh]$	12

Table 2. *Electric heat pump data*

The data of an electric heat pump are given in

Table 2. The primary energy required by a GSHP with a value of $SPER_{GSHP}=1.4$ can be calculated to provide the same heat as an EHP.

$$SPER_{GSHP} = \frac{Q_{HP}}{Q_p} \rightarrow Q_p = \frac{12}{1.4} = 8.57[kWh] \quad (7)$$

This means that the heat recovered from the environment in this heat pump is only 3.43 kWh:

$$Q_{C,GSHP} = Q_{HP} - Q_p = 12 - 8.57 = 3.43\ [kWh] \quad (8)$$

While the EHP, based on the data presented in

Table 2, recovers 8.57 kWh.

$$Q_{C,EHP} = Q_{HP} - W_{elec} = 12 - 3.43 = 8.57[kWh] \quad (9)$$

Therefore, even though both systems have the same PER and deliver the same amount of heat, the GSHP recovers 2.5 times less ambient energy than the EHP. This feature enables the reduction of the size and cost of the cold source, typically the ambient air. One of the disadvantages of this type of heat pump is its low coefficient of performance. The impact of the electrical consumption of the circulation pumps can influence the global efficiency [19]. Giorgio et al. [20] studied improving performance by regulating flow in the solution branch.
GEHP: In this kind of heat pump, the mechanical energy produced in an internal combustion engine drives the compressor. In other words, part of the chemical primary energy is converted to mechanical secondary energy

applied to the heat pump system and the rest as waste heat can be recovered in another system. The mechanical efficiency of an internal combustion engine is in the range of 30% to 45% [21]. Ease of modulation of the speed of the compressor by controlling the gas flow rate as well as the possibility of recovering the waste heat produced, make it possible to optimize the efficiency of the system**.** According to Pawela et al. due to the noise level they create, these systems should be placed outside and at a suitable distance to provide sound comfort [22]. It is obvious that when the engine speed increases, the heat produced by the heat pump at the level of the condenser increases as well as the waste heat which can be used to heat the DHW water and/or heating. This is why, in the calculation of performance, the impact of the waste heat must be considered. In this case, PER_{GEHP} can be calculated by following:

$$SPER_{GEHP} = SPF_{GEHP}.\eta_{mec} + \eta_{wh}.(1 - \eta_{mec}) \quad (10)$$

Where η_{mec} and η_{wh} are respectively the mechanical efficiency of the engine and the thermal efficiency to recover the waste heat. Like GSHP, a comparative analysis with an EHP makes it possible to evaluate a GEHP (Figure 4).

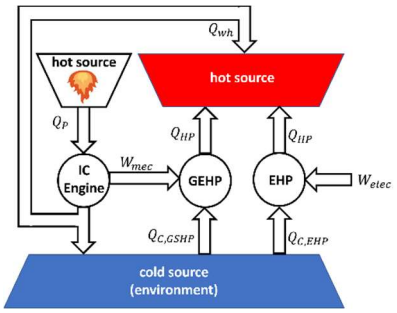

Figure 4. Schematic representation of GEHP and EHP.

Using the values for a GEHP performed in *Table 3*, one can compare with an EHP whose data is performed in

Table 2.

SPF_{GEHP}	4[22]
η_{mec}	35% [21]
η_{WH}	80% [21]

Table 3. Data of a GEHP

Substituting the numerical values into Eq.10 gives SPER:

$$SPER_{GEHP} = 4 \times 0.35 + 0.8 \times (1 - 0.35) = 1.92$$

Whereas for the electric heat pump studied, the PER is 1.4. This means that for the same primary energy consumption and the same heat recovered by the heat pump, the waste heat of the motor can be recovered in the system, thus obtaining an energy gain compared to an electric heat pump.

The disadvantages that can be referred to are the vibrations and movements associated with the transmission ratios of the motor shaft to the compressor shaft, the emission of noise, the need for regular maintenance treatments: oil change, replacement of oil and air filters, replacement of spark plugs [23].

GTHP: Gas driven thermal compression heat pump uses a compressor that works with thermal energy. The architecture of this compressor is identical to the Gamma type Stirling engine by removing the working piston and adding two valves for suction and discharge of the refrigerant. This compressor is designed by BOOSTHEAT to be integrated into a heat pump. The working principle of this compressor has been described by Rabah et al [24]. The compression system of a GTHP, including an external combustion engine, is limited to the use of nonflammable refrigerants, in particular CO_2. Considering that the mechanical work produced by a Stirling engine is completely converted into pressure work, the efficiency of the compressor and the Stirling engine are identical. If the mechanical efficiency of a Stirling engine is 40%, this means that 40% of the primary energy is used to drive the compression system (Figure 5).

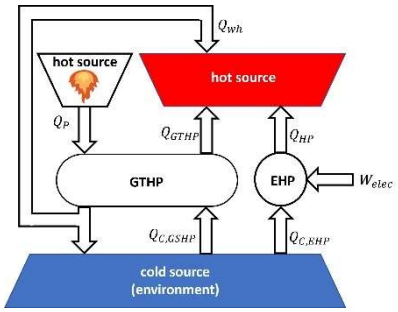

Figure 5. Schematic representation of GEHP and EHP.

In the following, the study of a GTHP operating with supercritical CO_2 allows an energy analysis of this type of heat pump.

III. Description of GTHP model

The installation studied is a three-stage compression heat pump system, where the refrigerant is CO_2, and the compressors are the thermal ones mentioned above. The fluid circuits and components of this heat pump are described in Figure 6. Note that the first and second stage compressors have their own burners, while the third stage is fueled by exhaust gases.

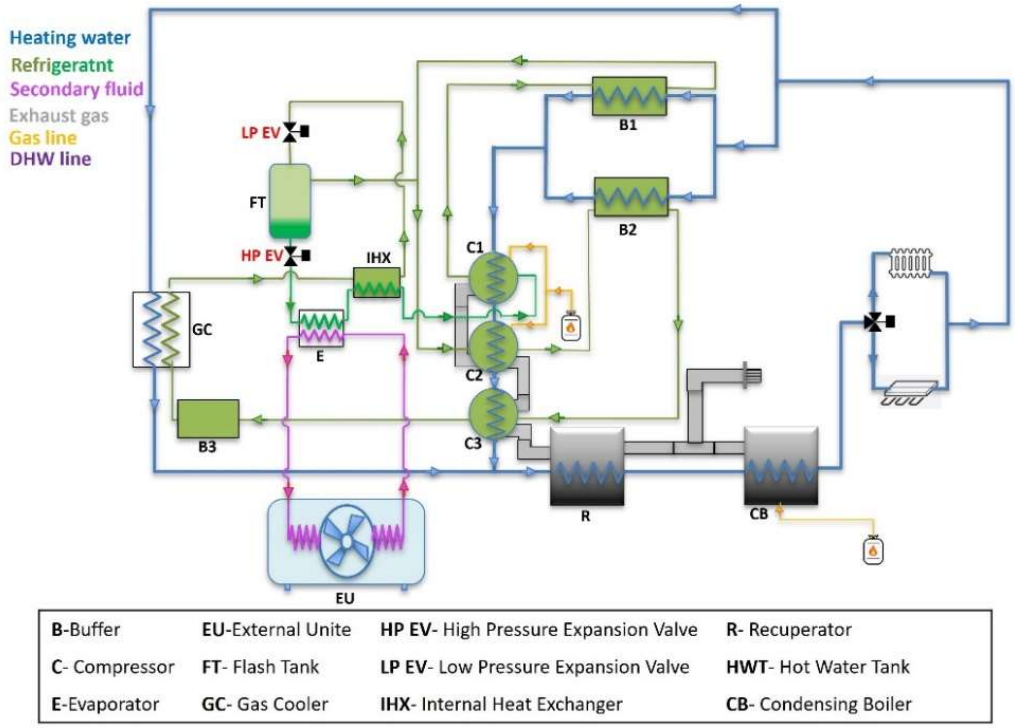

Figure 6.Heat pump schematic plan under study.

CO_2 leaving the evaporator is heated by internal heat exchanger (IHX) before being drawn in by a first stage compressor. At the compressor outlet, the CO_2 is cooled by the heating return water in buffer 1 before mixing with the saturated steam from the flash tank. Then all the refrigerant is compressed by the second stage and cooled by heat exchange with the return water in buffer 2. Finally, the CO_2 is sucked in by the third compressor. The CO_2 flow at the outlet of the last stage is stabilized by buffer 3 before entering the gas cooler (GC). At the GC, the supercritical CO_2 cools before entering the IHX where CO_2 from the GC heats CO_2 from the evaporator. The CO_2 leaving the GC expands in the high-pressure expansion valve (HP EV) and then enters the flash tank (FT) where the CO_2 separates into two parts liquid and saturated vapor, the saturated liquid expands in the low pressure expansion valve (LP EV) before entering the evaporator and the saturated vapor joins the CO_2 at the outlet of buffer 1 before being drawn in by compressor 2. The heating return water flows through buffers 1 and 2, reunites

and then enters the water exchangers of the thermal compressor, called water boxes, as a cold source. On the other hand, part of the heating return water goes to the gas cooler before being mixed with the water coming from the water boxes. To recover the heat from the exhaust gases, all the water goes to the heat recovery exchanger.
The Figure 7 shows the evolution of pressure as a function of specific energy (enthalpy) in this installation.

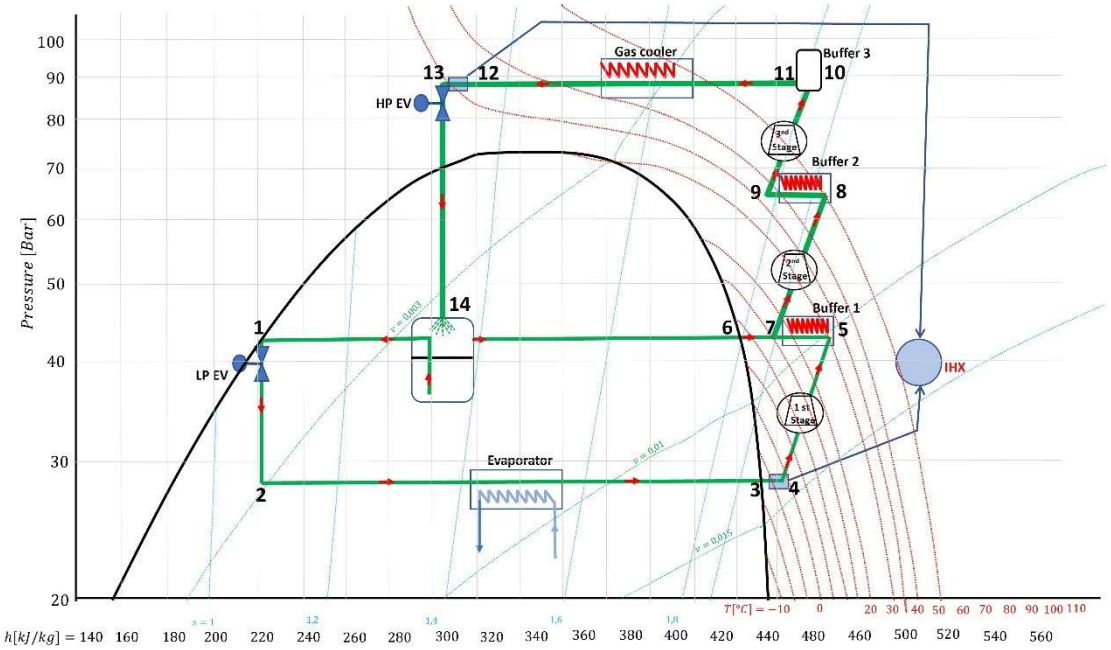

Figure 7.p-h diagram of the CO_2 transcritical cycle in the heat pump under study.

3-1-Performance strategy
In this study, the operating conditions of the system correspond to those defined by the European standard EN12309 [25] for an average climate. The power decreases linearly with the outside temperature, so that at a temperature of 16°C, there will be no need for heating. The Partial Load Ratio (PLR) and return water temperatures are defined as follows:

$$PLR = \frac{T_{ext,i}-16}{T_{design}-16}\% \tag{11}$$

$$T_{w,in} = T_{w,out} - \left(7 + \frac{T_{w,out}-35}{3}\right) \times 10 \tag{12}$$

Where $T_{w,in}$ and $T_{w,out}$ are the return and outlet temperatures of the system, respectively, and $T_{ext,i}$ is the outdoor temperature. The tests are differentiated according to two heating water flow temperatures defined as follows: low temperature (35°C, W35) and high temperature (55°C, W55). Part of the heat produced by this heat pump is caused by exhaust gas recuperation. On the other hand, at certain operating points, i.e., below the point F in standard EN12309 (Table 4), the thermal output supplied by the heat pump is not sufficient and an auxiliary boiler is required (CB in Figure 6).

Where $\dot{Q}_{HS}$ is the heat supplied by the GTHP and T_{ext} is the outdoor temperature in °C. As a result, to supply heat according to the EN12309 standard, it is necessary to add an auxiliary unit, which in this system is a condensing boiler. Table 4 shows the operating conditions of the system and the thermal output supplied by the heat pump and by the auxiliary heater when the nominal thermal power of the system is 16kW, which, according to the said standard, corresponds to an outside temperature of -10°C.

Conditions	T_{ext} [°C]	PRL [%]	EN12309 $T_{W,out}$ [°C]	EN12309 $T_{W,in}$ [°C]	EN12309 $T_{W,out}$ [°C]	EN12309 $T_{W,in}$ [°C]	$\dot{Q}_{HS}[kW]$		Auxiliary heat [kW]	
			W35		W55		W35	W55	W35	W55
E	-10	100	35	28	55	41,3	7,89	5,37	8,11	10,63
A	-7	88	34	27,3	52	39,3	8,86	6,14	5,29	6,14
F	0	62	30,9	25,3	44,2	40	9,91	8,48	-	1,36
B	2	54	30	24,7	42	32,7	8,62	8,62	-	-
C	7	35	27	22,7	36	28,7	5,54	5,54	-	-
D	12	15	24	20,7	30	24,7	2,46	2,46	-	-

Table 4. The operating conditions of the installation.

According to Table 4, the thermal output supplied by the heat pump is expressed by Eq.13 and Eq.14:

$$\dot{Q}_{HS} = 0{,}0175\ {T_{ext}}^2 + 0{,}0273\ T_{ext} + 9.9131 \text{ ; for W35} \quad (13)$$

$$\dot{Q}_{HS} = 0{,}0077\ T_{ext}^2 + 0{,}3884\ T_{ext} + 8.4838 \text{ ; for W55} \quad (14)$$

It is important to note that these two equations are only valid when the auxiliary is utilized. Otherwise, the installation will generate the same thermal power as indicated in the standard.

The CO_2 flow provided by the thermal compressors, varies according to two parameters: the temperature of the hot side (heater) and the speed of displacer. The selected control is of the PID type, which makes it possible to supply the cooling flow corresponding to the PRL with the heater temperature and the speed of the first stage motor. The temperature of second stage and the speeds of two other stages are controlled by the parameters of first stage.

3-2-Modelling

The modeling of the operation of the system is a result of all the models of the components of the installation. The thermodynamic properties of CO_2 are calculated using Coolprop[26]. The inputs and outputs of the model are shown in Figure 8.

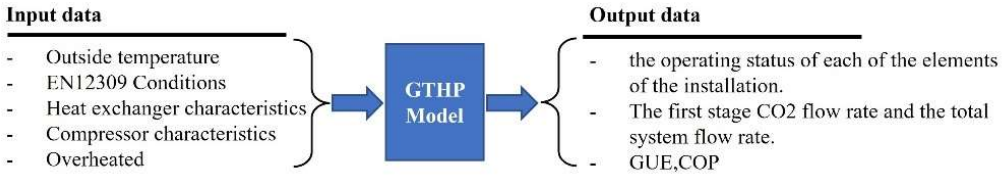

Figure 8. The inputs and outputs of the model.

The characteristics of the components used in the system make it possible to find the operating states of each process. These characteristics can be obtained either by modeling or by experimental methods.

The compressor model makes it possible to know the refrigerant flow rate and isentropic efficiency of the compressor. The idea of the thermal compressor describes that heat can be used to provide pressure and CO_2 moves between the cold source and the hot source through a displacer (Figure 9). This is a compressor invented by BOOSTHEAT. Its architecture is identical to that of a Gamma-type Stirling engine, except that the working piston and the cylinder are replaced by two valves. This compressor consists of a cylinder, a displacer piston (D), a heater (H), a regenerator heat exchanger (R), a cooler (K), an inlet valve (IV) and an exhaust valve (EV).

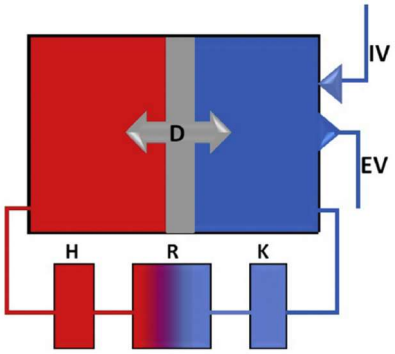

Figure 9. Concept of Thermal compressor.[24]

The pressure variation across the compressor can be viewed as a periodic function at constant speed. The amplitude of this periodic function increases progressively with temperature. When the temperature is high enough so that the discharge set pressure can be reached, the discharge valve can open and a quantity of gas will come out of the compressor, causing the pressure to drop, so the inlet valve opens, and the gas enters the compressor. The mass of gas in the compressor can be studied in two conditions: first, just before the exhaust valve opens (m_{EV}) and second, just before the inlet valve opens (m_{IV}).

$$m_{EV} = (\sum_i m_i)_{EV} \tag{15}$$

$$m_{IV} = (\sum_i m_i)_{IV} \tag{16}$$

Where i is the control volume index, including the compression (C), expansion (E), and dead volume parts (D: cooler, regenerator, and heater). Assuming that CO_2 is like an ideal gas, then:

$$m_{EV} = \left(P \frac{M}{R} \left(\frac{V_C}{T_C} + \frac{V_E}{T_E} + \sum \frac{V_D}{T_D} \right) \right)_{EV} \tag{17}$$

$$m_{IV} = \left(P \frac{M}{R} \left(\frac{V_C}{T_C} + \frac{V_E}{T_E} + \sum \frac{V_D}{T_D} \right) \right)_{IV} \tag{18}$$

The difference between these two masses during the time before opening and after closing the exhaust valve is the flow rate.

$$m_{comp} = m_{EV} - m_{EV} \tag{19}$$

$$m_{comp} = P_{asp} \frac{M}{R} \left(\frac{V_C}{T_C} - \tau \frac{V_E}{T_E} - (\tau - 1) \sum \frac{V_D}{T_D} \right) \tag{20}$$

Where m_{comp} is the suction and discharge mass of the compressor and τ is the pressure ratio:

$$\tau = {P_{dis}}/{P_{asp}} \tag{21}$$

Where P_{dis} and P_{asp} are discharge pressure and aspiration pressure, respectively.

The inlet and outlet masses of the fluid and the masse of compressed CO_2 are determined according to the model of Rabah et al.[24]. Figure 10 shows the result for one operating point.

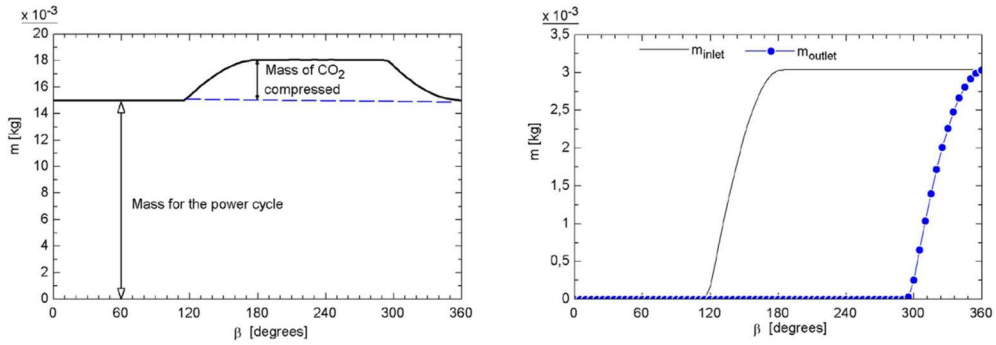

Figure 10. Inlet and outlet mass of fluid per cycle and mass of compressed[24].

The low pressure is saturation pressure of evaporation temperature T_{evap},which is determined from the outdoor temperature and the efficiency of the E and EU exchangers (see Figure 6).

$$T_{evap} = f(T_{ext}, \varepsilon_E, \varepsilon_{EU}) \quad (22)$$

The outlet temperature of the gas cooler is a function of the thermal efficiency of the gas cooler and the temperature of the heating water returning to the system.

$$T_{gc,out,d} = f(T_{W,in}, \varepsilon_{gc}) \quad (23)$$

The high pressure of the cycle is defined by the outlet temperature of the gas cooler:

$if\ T_{gc,out,d} < 31\,°C \Longrightarrow HP = P_{sat}$

$if\ T_{gc,out,d} > 31\,°C \Longrightarrow HP = HP_{opt}$

Where P_{sat} is the saturation pressure of CO_2 at $T_{gc,out,d}$. In this case, the cycle is subcritical, and condensation occurs. In the case of the transcritical cycle, the optimum pressure at the high-pressure level is defined by Eq.15 [27].

$$HP_{opt} = (2{,}778 - 0{,}0157\,T_{evap}).\,T_{gc,out,d} + (0{,}381.T_{evap} - 9{,}34) \quad (24)$$

Where HP_{opt} is the optimum pressure in bar and the evaporation temperature in °C, respectively.

The intermediate pressures of the stages can be estimated using the following equation:

$$IP_i = i \times \frac{(HP_{opt} - LP)}{n} + LP \quad (25)$$

Note that *i* is stage number and *n* is the total number of stages. However, the model's intermediate pressures are modified because of compression rate constraints. To calculate the temperature of the CO_2 leaving the gas cooler,$T_{gc,out}$, the flow rate of the first stage, $\dot{m}_{1,init}$, is initiated. This allows for the calculation of the total flow rate, $\dot{m}_{tot}$.

$$\dot{m}_{tot} = \dot{m}_1 + \dot{m}_6 \quad (26)$$

The output flow rate of the flash tank on the steam side,$\dot{m}_6$, could be estimated by using of vapor quality definition:

$$x_{th} = \frac{\dot{m}_6}{\dot{m}_{tot}} = \frac{h_{14} - h_1}{h_6 - h_1} \quad (27)$$

This allows for the calculation of the total flow rate, $\dot{m}_{tot}$.

$$\dot{m}_{tot} = \dot{m}_1 \left(\frac{h_6 - h_1}{h_6 - h_{14}}\right) \quad (28)$$

The enthalpies of the points in the equation are obtained from their respective thermodynamic properties.

From the characteristics of the compressors and buffers in the installation, it is possible to estimate the enthalpy output from the gas cooler, h_{11}.

Thus, by carrying out the first law of thermodynamics on the gas cooler, the enthalpy output from this exchanger (h_{12}) can be calculated.

$$h_{12} = h_{11} - \frac{[\dot{m}.cp.\Delta T]_{water}}{\dot{m}_{tot}} \quad (29)$$

So, the temperature of the CO_2 leaving the gas cooler can be determined:

$$T_{gc,out} = f(HP_{opt}, h_{12}) \quad 30)$$

By comparing the calculated temperature of the CO_2 leaving the gas cooler $T_{gc,out}$ with the desired temperature at this point $T_{gc,out,d}$, the initial flow rate of the first stage can be modified.

If $T_{gc,out,d} > T_{gc,out} \Longrightarrow \dot{m}_1 = \dot{m}_1 + \Delta\dot{m}$

If $T_{gc,out,d} < T_{gc,out} \Longrightarrow \dot{m}_1 = \dot{m}_1 - \Delta\dot{m}$

Where $\Delta\dot{m}$ is the precision of the calculation. Until the point of convergence is reached, the calculations should be repeated.

The model will be validated by comparing the modelling results to the test measurements (Figure 15).

It is useful to note that to define the COP, the thermal powers exchanged between the primary fluid of the cycle (CO_2) and the secondary fluids at the cycle must be considered. Thus, the net heat supplied per thermodynamic cycle, $\dot{Q}_{H,cycl}$, then COP and GUE are calculated as follows:

$$\dot{Q}_{H,cycl} = \sum_{i=1}^{2} \dot{Q}_{B,i} + \sum_{i=1}^{3} \dot{Q}_{WB,i} + \dot{Q}_{gc} \quad (31)$$

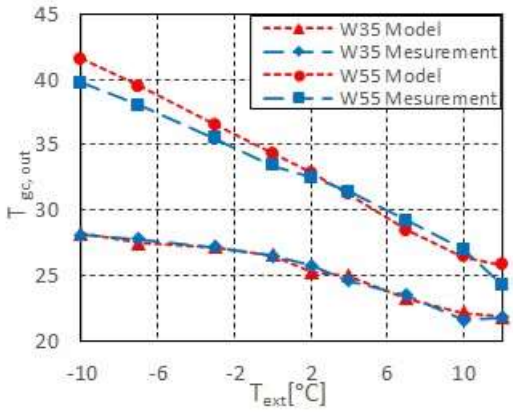

Figure 11. Comparison between measurements and results of the model.

$$COP = \frac{\dot{Q}_{H,cycl}+\dot{Q}_{H,exhau}}{\dot{Q}_{Gas}+\frac{\dot{W}_{elec}}{\eta_{tot}}} \quad (32)$$

$$GUE = \frac{\dot{Q}_{H,cycl}+\dot{Q}_{H,exhaust}}{\dot{Q}_{Gas}} \quad (33)$$

Where $\dot{Q}_B$, $\dot{Q}_{WB}$, $\dot{Q}_{gc}$ and $\dot{Q}_{H,exhaust}$ are the heat recovered in buffers, water boxes, gas cooler and heat recovered from exhaust gases respectively. $\dot{W}_{elec}$ is electric power consumption for the movement of the compressor displacer. Also $\dot{Q}_{evap}$ is evaporator heat exchange and $\dot{Q}_{Gas}$ is natural gas heat value.

The model has been validated by tests carried out on the installation at various points of operation.

3-Results and discussion

The model developed allows to evaluate the installation from the point of view of optimal operation; thanks to the graphical interface of the model, for each operating point, the thermodynamic characteristics of the cycle and the energetic characteristics are visible.

According to Table 4, an auxiliary is necessary for the installation to meet the additional thermal requirements at low temperatures. Without the auxiliary, operation will be possible from 0°C in the W35 regime and from 2°C in the W55 regime, as shown in Figure 12.

It is obvious that at low temperature points where the pressure ratio is very high, the flow rate is lower and therefore the compressor operates at full load, i.e., at maximum heater temperature (Figure 13a). As the pressure ratio decreases, the flow rate increases.

Figure 12. The heat supplied by TDHP for two operating modes.

However, as the heat demand decreases, the temperature of the heater also decreases, resulting in a reduction in CO_2 flow. The pressure difference across the piston increases at lower temperatures, resulting in a higher electric power demand to maintain the same speed. The Figure 13(b) illustrates the fluctuations in the rotational speed of the initial stage.

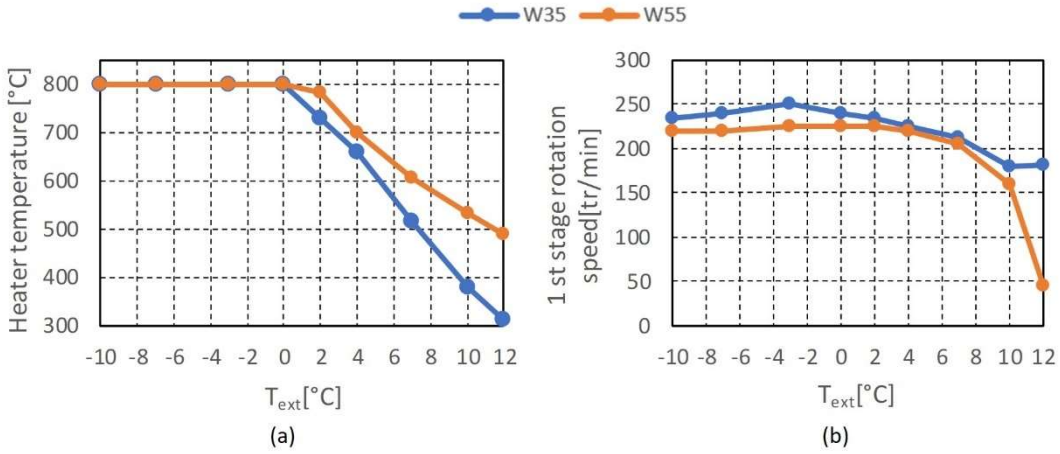

Figure 13. (a) Heater temperature evolution, (b) 1st stage rotation speed evolution

The CO2 flow variation, obtained by modeling is shown in Figure 14 .

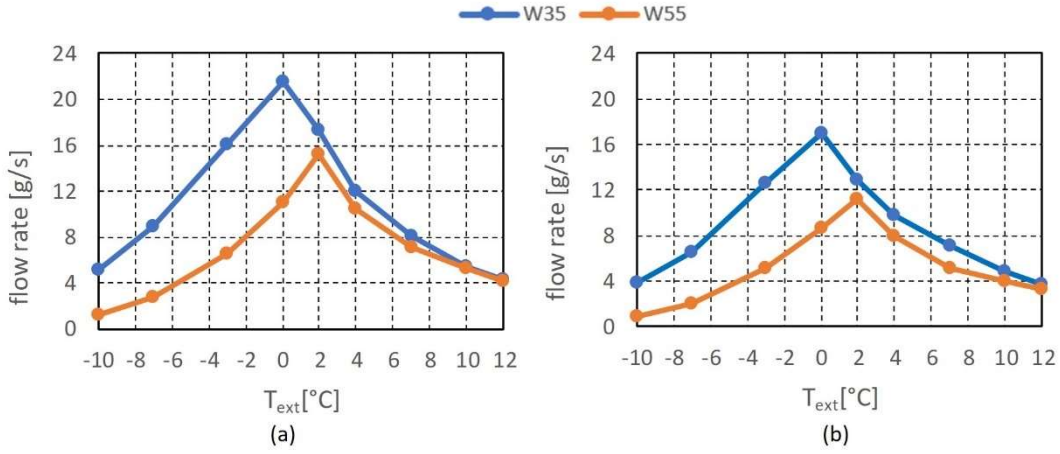

Figure 15. CO2 flow rate variation in (a) 1st stage (b) 3rd stage

The values of COP and GUE can be estimated from equations 32 and 33, the values of GUE and COP can be estimated. Figure 14a and Figure 14b show the values of COP and GUE for each operating point.

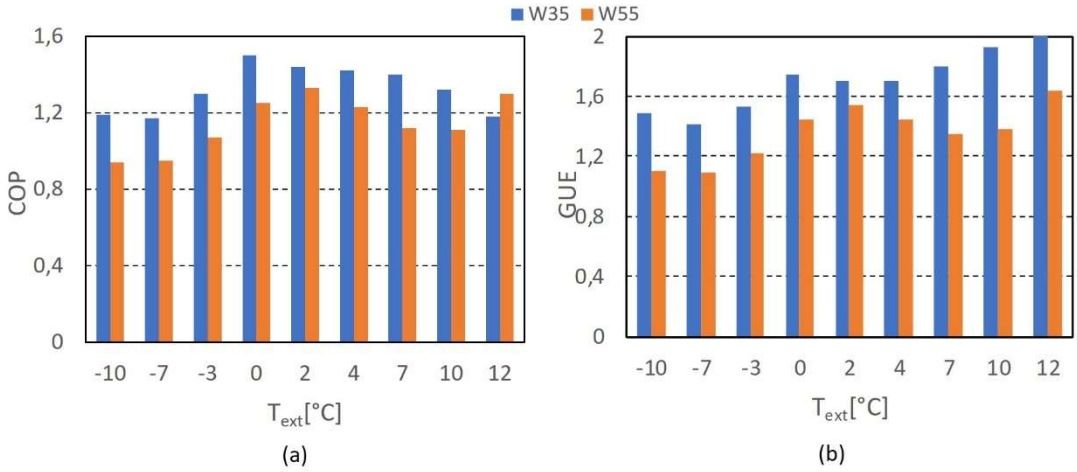

Figure 16. (a) GUE (b) COP

The method used to calculate SGUE is that proposed by EN 12309 [28].

$$SGUE = \frac{\sum_{j=1}^{N} h_j \times \dot{Q}_{H,total}(T_j)}{\sum_{j=1}^{N} h_j \times \frac{\dot{Q}_{H,total}(T_j)}{GUE(T_j)}} \quad (34)$$

Where h_j is the HP operating hours when the outdoor temperature is T_j, and $\dot{Q}_{H,total}$ is the total heat recovered by the system, which includes $Q_{H,cycl}$ and $Q_{H,exhaust}$. Table 5 shows the results of the SGUE calculation for two operating modes.

Operating modes	SGUE
W35	1.7
W55	1.4

Table 5. SGUE for two operating modes of TDHP

Equation 32 describes that the COP of the thermal compression heat pump is equal to PER and therefore, according to the mentioned standard, The SPER can be calculated, which allows a comparison with an electric heat pump. The results of the SPER calculation for two operating modes (W35 and W55) are summarized in Table 6.

Operating modes	SPER
W35	1.33
W55	1.19

Table 6. Seasonal Primary Energy Ratio of TDHP

According to Eq. 4, the SPF or SCOP of an electric heat pump can be estimated under conditions identical to those of the GTHP (Table 7).

Operating modes	SPF (or SCOP)
W35	3.32
W55	3

Table 7. Seasonal Coefficient of Performance of EHP

Note that in Eq.4, according to the EN12309 standard, the value adopted for η_{tot} is 40%.
According to Figure 5, the amount of heat recovered from the environment, Q_C, to produce the same quantity of heat by an EHP and a GTHP is determined:

$$Q_{C,EHP} = Q_{HP} - \frac{Q_H}{SPF} \quad (35)$$

$$Q_{C,GTHP} = Q_{HP} - \frac{Q_H}{SPER} \quad (36)$$

Results for $Q_{HP} = 12\ kWh$ are shown in Table 8.

Operating modes	$Q_{C,EHP}$ [kWh]	$Q_{C,GTHP}$ [kWh]
W35	8.4	3
W55	8	2

Table 8. The ambient energy recovered by EHP and GTHP

Therefore, even though both systems have the same PER and the same amount of heat output, the amount of ambient energy recovered by GTHP is more than 2.5 time (W35) and 4 times (mode W55) less than that of the EHP. This feature enables a reduction in the size and cost of the cold source, typically ambient air.

IV. Conclusion

The interest of this study is the evaluation of a thermal compression heat pump operating with CO_2. The prediction of system behavior through modeling is complemented with experimental tests to know the real behavior of the system, which makes it possible to clarify the operation of this type of compressor in a configuration of a heat pump. The results show that this type of compressor has advantages and potentials that encourage spending time to improve its operation. The increase in compression efficiency is a function of the compressor architecture, specifically the increase in the efficiency of the heat exchange between a heat source and

CO_2. Another advantage of the thermal compressor is its ability to utilize waste heat. Studies on the configuration and components of the cycle are another way to increase the performance of the TDHP.

References

[1]. E. A. Heath, "Amendment to the Montreal Protocol on Substances that Deplete the Ozone Layer (Kigali Amendment)," International Legal Materials, vol. 56, no. 1, pp. 193–205, 2017, doi: 10.1017/ilm.2016.2.

[2]. N. Abas, A. R. Kalair, N. Khan, A. Haider, Z. Saleem, and M. S. Saleem, "Natural and synthetic refrigerants, global warming: A review," Renewable and Sustainable Energy Reviews, vol. 90, pp. 557–569, 2018, doi: https://doi.org/10.1016/j.rser.2018.03.099.

[3]. Y. Heredia-Aricapa, J. M. Belman-Flores, A. Mota-Babiloni, J. Serrano-Arellano, and J. J. García-Pabón, "Overview of low GWP mixtures for the replacement of HFC refrigerants: R134a, R404A and R410A," International Journal of Refrigeration, vol. 111, pp. 113–123, 2020, doi: https://doi.org/10.1016/j.ijrefrig.2019.11.012.

[4]. J. D. Rogers and R. D. Stephens, "Absolute infrared intensities for F-113 and F-114 and an assessment of their greenhouse warming potential relative to other chlorofluorocarbons," J Geophys Res, vol. 93, pp. 2423–2428, 1988.

[5]. D. A. Fisher, C. H. Hales, W.-C. Wang, M. K. W. Ko, and N. D. Sze, "Model calculations of the relative effects of CFCs and their replacements on global warming," Nature, vol. 344, no. 6266, pp. 513–516, Apr. 1990, doi: 10.1038/344513a0.

[6]. L. Cecchinato, M. Corradi, E. Fornasieri, and L. Zamboni, "Carbon dioxide as refrigerant for tap water heat pumps: A comparison with the traditional solution," International Journal of Refrigeration, vol. 28, no. 8, pp. 1250–1258, 2005, doi: https://doi.org/10.1016/j.ijrefrig.2005.05.019.

[7]. G. Lorentzen, "Revival of carbon dioxide as a refrigerant," International Journal of Refrigeration, vol. 17, no. 5, pp. 292–301, Jan. 1994, doi: 10.1016/0140-7007(94)90059-0.

[8]. M.-H. Kim, J. Pettersen, and C. W. Bullard, "Fundamental process and system design issues in CO2 vapor compression systems," Prog Energy Combust Sci, vol. 30, no. 2, pp. 119–174, 2004, doi: https://doi.org/10.1016/j.pecs.2003.09.002.

[9]. P. Munshi and S. Bhaduri, "Supercritical CO2: A twenty-first century solvent for the chemical industry," Curr Sci, vol. 97, Jul. 2009.

[10]. M. A. 'McHugh and V. J. 'Krukonis, Supercritical Fluid Extraction. Elsevier, 1994. doi: 10.1016/C2009-0-26919-4.

[11]. J. 'Staub, "CO2 As Refrigerant: The Transcritical Cycle," 2004, Accessed: Jul. 12, 2023. [Online]. Available: https://www.achrnews.com/articles/94092-co2-as-refrigerant-the-transcritical-cycle

[12]. Y. Ma, Z. Liu, and H. Tian, "A review of transcritical carbon dioxide heat pump and refrigeration cycles," Energy, vol. 55, pp. 156–172, 2013, doi: https://doi.org/10.1016/j.energy.2013.03.030.

[13]. A. Cavallini and C. Zilio, "Carbon dioxide as a natural refrigerant," International Journal of Low-Carbon Technologies, vol. 2, no. 3, pp. 225–249, Jul. 2007, doi: 10.1093/ijlct/2.3.225.

[14]. Y. Wang, Y. He, Y. Song, X. Yin, F. Cao, and X. Wang, "Energy and Exergy Analysis of the Air Source Transcritical CO2 Heat Pump Water Heater Using CO2-Based Mixture as Working Fluid," Energies (Basel), vol. 14, no. 15, p. 4470, Jul. 2021, doi: 10.3390/en14154470.

[15]. L. Chamra and P. Mago, "Micro-CHP power generation for residential and small commercial buildings," Micro-CHP Power Generation for Residential and Small Commercial Buildings, pp. 1–82, Jul. 2008.

[16]. P. Maina and Z. Huan, "A review of carbon dioxide as a refrigerant in refrigeration technology," S Afr J Sci, vol. 111, Jul. 2015, doi: 10.17159/sajs.2015/20140258.

[17]. L. F. Cabeza, A. Solé, and C. Barreneche, "Review on sorption materials and technologies for heat pumps and thermal energy storage," Renew Energy, vol. 110, pp. 3–39, Sep. 2017, doi: 10.1016/j.renene.2016.09.059.

[18]. R. Nouvel, M. Cotrado Sehgelmeble, and D. Pietruschka, "European Mapping of Seasonal Performances of Air-source and Geothermal Heat Pumps for Residential Applications," Jul. 2015.

[19]. M. Fumagalli, A. Sivieri, M. Aprile, M. Motta, and M. Zanchi, "Monitoring of gas driven absorption heat pumps and comparing energy efficiency on primary energy," Renew Energy, vol. 110, pp. 115–125, 2017, doi: https://doi.org/10.1016/j.renene.2016.12.058.

[20]. G. Villa, T. Toppi, M. Aprile, and M. Motta, "Performance improvement of gas-driven absorption heat pumps by controlling the flow rate in the solution branch," International Journal of Refrigeration, vol. 145, pp. 290–300, 2023, doi: https://doi.org/10.1016/j.ijrefrig.2022.09.015.

[21]. A. Hepbasli, Z. Erbay, F. Icier, N. Colak, and E. Hancioglu, "A review of gas engine driven heat pumps (GEHPs) for residential and industrial applications," Renewable and Sustainable Energy Reviews, vol. 13, no. 1, pp. 85–99, 2009, doi: https://doi.org/10.1016/j.rser.2007.06.014.

[22]. B. Pawela and M. Jaszczur, "Review of Gas Engine Heat Pumps," Energies (Basel), vol. 15, p. 4874, Jul. 2022, doi: 10.3390/en15134874.

[23]. A. Rucinski, A. Rusowicz, and A. Grzebielec, "Gas engine driven heat pump – characteristics, analysis of applications in buildings energy systems," in The 9th International Conference "Environmental Engineering 2014," Vilnius, Lithuania: Vilnius Gediminas Technical University Press "Technika" 2014, 2014. doi: 10.3846/enviro.2014.280.

[24]. R. Ibsaine, J. M. Joffroy, and P. Stouffs, "Modelling of a new thermal compressor for supercritical CO2 heat pump," Energy, vol. 117, pp. 530–539, Dec. 2016, doi: 10.1016/j.energy.2016.07.017.

[25]. European standard, "EN12309 gas-fired sorption appliances for heating and/or cooling with a net heat input not exceeding 70kW," 2014.

[26]. I. H. Bell, J. Wronski, S. Quoilin, and V. Lemort, "Pure and Pseudo-pure Fluid Thermophysical Property Evaluation and the Open-Source Thermophysical Property Library CoolProp," Ind Eng Chem Res, vol. 53, no. 6, pp. 2498–2508, 2014, doi: 10.1021/ie4033999.

[27]. S. M. Liao, T. S. Zhao, and A. Jakobsen, "A correlation of optimal heat rejection pressures in transcritical carbon dioxide cycles," Appl Therm Eng, vol. 20, no. 9, pp. 831–841, Jun. 2000, doi: 10.1016/S1359-4311(99)00070-8.

[28]. EN 12309–4: 2014: "Gas-fired sorption appliances for heating and/or cooling with a net heat input not exceeding 70 kW."